npj | Quantum Information

www.nature.com/npjqi

ARTICLE OPEN

Less entanglement exhibiting more nonlocality with noisy measurements

Gaoyan Zhu[1], Daniel Dilley[2], Kunkun Wang[1], Lei Xiao[1], Eric Chitambar[3] and Peng Xue[1]✉

The Clauser–Horne–Shimony–Holt (CHSH) inequality test is widely used as a mean of invalidating the local deterministic theories. Most attempts to experimentally test nonlocality have presumed unphysical idealizations that do not hold in real experiments, namely, noiseless measurements. We demonstrate an experimental violation of the CHSH inequality that is free of idealization and rules out local models with high confidence. We show that the CHSH inequality can always be violated for any nonzero noise parameter of the measurement. Intriguingly, less entanglement exhibits more nonlocality in the CHSH test with noisy measurements. Furthermore, we theoretically propose and experimentally demonstrate how the CHSH test with noisy measurements can be used to detect weak entanglement on two-qubit states. Our results offer a deeper insight into the relation between entanglement and nonlocality.

npj Quantum Information (2021)7:166 ; https://doi.org/10.1038/s41534-021-00506-y

INTRODUCTION

Quantum systems exhibit a wide range of non-classical and counter-intuitive phenomena, such as quantum entanglement[1] and Bell nonlocality[2]. Bell's inequality fundamentally provides a wealth of understanding in what differentiates the classical from the quantum world. Bell's insight that nonlocal correlations between quantum systems cannot be explained classically can be verified experimentally and has numerous applications in modern quantum information[3–8]. A great effort has also been devoted to understanding the relation between entanglement and nonlocality[9–22]. A fundamental problem with most proposals[13–15] for testing nonlocality and experiments[23–27] performed to date, is that measurements are assumed to have a deterministic response in the nonlocality model. It has been shown that this can only be justified under the idealization, namely, noiseless measurements[28]. For Bell's notion of local causality, the theoretical work by Clauser et al.[29] is critical to enabling an experimental test without unphysical idealizations, i.e., without the perfect anti-correlation presumed in Bell's original proof. Furthermore, Dilley and Chitambar[30] show how to devise the test that is free of the other idealization that measurements are noiseless, which is never satisfied precisely by any real experiment. They consider a scenario in which one party has inefficient detectors and can only perform noisy measurements and show that the Clauser–Horne–Shimony–Holt (CHSH) inequality can always be violated for measurements with any nonzero detection efficiency.

In this work, we perform an experimental violation of the CHSH inequality under a scenario when one party performs noisy measurements, which is known as an asymmetric Bell experiment. It should be mentioned that in our experiments the loopholes of a Bell test are not closed which requires extremely high experimental costs and rigorous technology[31–34]. First, we consider a range of non-maximal two-qubit entangled states and show that the CHSH inequality can always be violated for any nonzero noise parameter of the measurement. Surprisingly, less entanglement exhibits more nonlocality in the CHSH test with noisy measurements. Furthermore, as an application of the CHSH test with noisy measurements, we show how it is possible to also detect the presence of weak entanglement of a two-qubit system. Our results offer a thorough understanding of the relation between entanglement and nonlocality.

RESULTS

Theoretical scenarios

First, consider a hybrid scenario in which Alice and Bob share a two-qubit state. Alice's detector has perfect efficiency and she can perform an ideal measurement, while Bob can only perform a noisy measurement which has a conclusive detection only a fraction η of the time. Alice randomly chooses to measure her qubit in the direction $\hat{a}_x$ ($x = 0, 1$) and the outcome a is denoted by either 0 or 1. The projector for Alice's measurement is

$$\Pi^A_{a|x} = \frac{1}{2}[\mathbb{1} + (-1)^a \hat{a}_x \cdot \hat{\sigma}], \tag{1}$$

where $\hat{\sigma} = \sigma_x\hat{x} + \sigma_y\hat{y} + \sigma_z\hat{z}$ is a vector of Pauli matrices. In a realistic setup, it might not be possible to obtain a conclusive measurement outcome. We consider a simple scenario, where an inconclusive outcome can only arise on Bob's measurements, occurring with frequency $(1-\eta)$ for both of his measurement choices. Thus, Bob performs a positive operator-valued measure (POVM) with two outcomes

$$\begin{aligned} \tilde{\Pi}^B_{0|y} &= \tfrac{\eta}{2}(\mathbb{1} + \hat{b}_y \cdot \hat{\sigma}) + (1-\eta)\mathbb{1}, \\ \tilde{\Pi}^B_{1|y} &= \tfrac{\eta}{2}(\mathbb{1} - \hat{b}_y \cdot \hat{\sigma}), \end{aligned} \tag{2}$$

where $\hat{b}_y$ ($y = 0, 1$) is the direction of Bob's measurement. The term $(1-\eta)\mathbb{1}$ corresponds to the inconclusive outcome.

The CHSH inequality with detection efficiency η on Bob's measurement is

$$2 \geq |E(0,0) + E(0,1) + E(1,0) - E(1,1)| = |\mathrm{Tr}(\rho\mathcal{B}_1)|, \tag{3}$$

[1]Beijing Computational Science Research Center, Beijing 100084, China. [2]Department of Physics and Astronomy, Southern Illinois University, Carbondale, IL 62901, USA. [3]Department of Electrical and Computer Engineering, Coordinated Science Laboratory, University of Illinois at Urbana-Champaign, Urbana, IL 61801, USA. ✉email: gnep.eux@gmail.com

where

$$E(x,y) := \sum_{a,b=0}^{1} f(a,b)p(a,b|x,y) = \mathrm{Tr}\,(\rho O_x^A \otimes O_y^B) \tag{4}$$

is the expected value of the nonlocal function $f(a, b) = (-1)^{a\oplus b}$ computed from the measurement outcomes, and the Bell operator for this scenario is

$$\mathcal{B}_1 = O_0^A \otimes (O_0^B + O_1^B) + O_1^A \otimes (O_0^B - O_1^B) \tag{5}$$

with the observables $O_x^A = \Pi_{0|x}^A - \Pi_{1|x}^A$ and $O_y^B = \tilde{\Pi}_{0|y}^B - \tilde{\Pi}_{1|y}^B$.

Without loss of generality, we choose the directions of Alice and Bob as

$$\begin{aligned} &\hat{a}_0 = \hat{z}, \hat{a}_1 = \cos\theta_A\hat{x} + \sin\theta_A\hat{z}, \\ &\hat{b}_0 = \hat{z}, \hat{b}_1 = \cos\theta_B\hat{x} + \sin\theta_B\hat{z}. \end{aligned} \tag{6}$$

The Bell operator then becomes

$$\begin{aligned} \mathcal{B}_1 &= \sum_{i,j\in\{x,z\}} c_{ij}\sigma_i \otimes \sigma_j + r_z\sigma_z \otimes \mathbb{1} \\ &= \eta\mathcal{B}_{\mathrm{CHSH}} + 2(1-\eta)\sigma_z \otimes \mathbb{1}, \end{aligned} \tag{7}$$

where

$$\begin{aligned} &r_z = 2(1-\eta), c_{xx} = -\eta\cos\theta_A\cos\theta_B, \\ &c_{xz} = \eta\cos\theta_A(1-\sin\theta_B), c_{zx} = \eta\cos\theta_B(1-\sin\theta_A), \\ &c_{zz} = \eta(1+\sin\theta_A+\sin\theta_B-\sin\theta_A\sin\theta_B), \end{aligned}$$

and $\mathcal{B}_{\mathrm{CHSH}}$ is the standard Bell operator with $\eta = 1$.

It is proven in ref. [30] that in a two-qubit CHSH test with detection efficiency η for one party and a perfect efficiency for the other, there exist measurement directions $\{\hat{a}_0, \hat{a}_1, \hat{b}_0, \hat{b}_1\}$ and a corresponding entangled state ρ such that the CHSH inequality is violated, i.e., $\mathrm{Tr}\,(\rho\mathcal{B}_1) > 2$ if $\eta > 1/2$. To analyze the entanglement in the state violating the CHSH inequality, if $\mathrm{Tr}\,(\rho\mathcal{B}_1) > 2(1+\kappa)$ for any $\kappa = \eta - 1/2 \geq 0$, the squared concurrence of the state ρ is then

$$\begin{aligned} C^2(\rho) < &\frac{(2\eta-1)[\kappa(2+\kappa)+2\eta(1-\eta)]}{(1-2\eta+2\eta^2)^2} \\ &+ \frac{2\eta(1-\eta)(1+\kappa)\sqrt{1-\kappa(2+\kappa)-4\eta(1-\eta)}}{(1-2\eta+2\eta^2)^2}. \end{aligned} \tag{8}$$

For any pure state which satisfies $C^2(\rho) = \kappa(2+\kappa)$, there exist suitable measurement directions to obtain the value of the CHSH inequality $\mathrm{Tr}\,(\rho\mathcal{B}_1) = 2(1+\kappa)$. For $\eta = 1$, as the states are more entangled the violation of the CHSH inequality becomes larger. Surprisingly, for $1/2 < \eta < 1$, more nonlocality with less entanglement is shown as the detection efficiency decreases[30].

Next, we consider the second scenario, which involves detection inefficiency for only one of Bob's measurement choices. That is, for $y = 1$, Bob performs a POVM $\{\tilde{\Pi}_{0|1}^B, \tilde{\Pi}_{1|1}^B\}$(2), while for $y = 0$, Bob performs a projective measurement $\Pi_{b|0}^B = [\mathbb{1} + (-1)^b\hat{b}_0 \cdot \hat{\sigma}]/2$(1). The corresponding Bell operator for the second scenario is then given by

$$\mathcal{B}_2 = \sum_{i,j\in\{x,z\}} c_{ij}\sigma_i \otimes \sigma_j + (r_x\sigma_x + r_z\sigma_z) \otimes \mathbb{1}, \tag{9}$$

where

$$\begin{aligned} &r_x = -(1-\eta)\cos\theta_A, r_z = (1-\eta)(1-\sin\theta_A), \\ &c_{xx} = -\eta\cos\theta_A\cos\theta_B, c_{xz} = \cos\theta_A(1-\eta\sin\theta_B), \\ &c_{zx} = \eta\cos\theta_B(1-\sin\theta_A), \\ &c_{zz} = 1+\eta\sin\theta_B+\sin\theta_A(1-\eta\sin\theta_B). \end{aligned}$$

It is shown in ref. [30] that in the second scenario, there exists a state ρ such that $\mathrm{Tr}\,(\rho\mathcal{B}_2) > 2$ for any $\eta > 0$ and any set of measurement directions $\{\hat{a}_0, \hat{a}_1, \hat{b}_0, \hat{b}_1\}$ with $\hat{a}_0 \neq \pm\hat{a}_1$ and $\hat{b}_0 \neq \pm\hat{b}_1$.

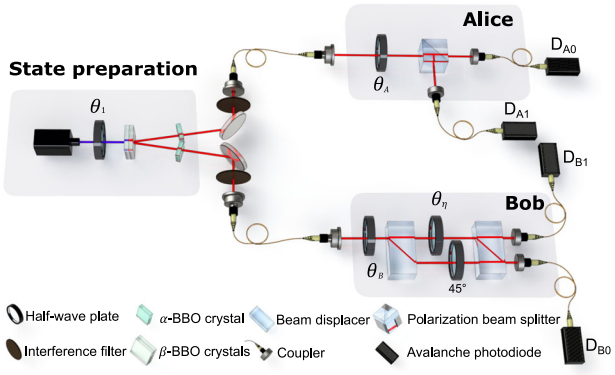

Fig. 1 Experimental setup. Desired quantum states are generated via type-I spontaneous parametric down-conversion using two joint β-Barium Borate (BBO) crystals. In the measurement stage, a half-wave plate (HWP) at θ_A and a polarizing beam splitter (PBS) on Alice's side perform the perfect projective measurement. For Bob's side, a POVM is performed by an HWP at θ_B and a Mach–Zehnder interferometer with two beam displacers (BDs) and two HWPs at θ_η and 45° inserted in each arm of the interferometer, respectively. For the second scenario, BDs and two HWPs are removed from the setup and an HWP at θ_B is used to perform a projective measurement instead of a POVM. Here the noisy parameter of POVM η is adjusted by tuning the setting angle of the HWP as $\theta_\eta = \arccos\sqrt{\eta}/2$.

Comparing these two scenarios, the first one guarantees the existence of some measurement directions that generate nonlocal correlations for $\eta > 1/2$ and places an upper bound on the entanglement needed to violate the CHSH inequality. In contrast, the second scenario says that any measurement direction will do and also has implications for the relationship between nonlocality and measurement incompatibility. For any two non-commuting observables on Alice's side, nonlocality can always be demonstrated using incompatible POVMs on Bob's side in which one of them is any standard observable and the other is any non-commuting "coarse-grained" observable, i.e., having the form of Eq. (2).

Experimental violation of the CHSH inequality with noisy measurements

We experimentally test the CHSH inequality without unphysical idealization—noiseless measurements. The experimental setup illustrated in Fig. 1, consists of an entangled photon source, entangled state preparation, and polarization measurement[35]. By using two adjacent nonlinear crystals (β-barium borate, BBO) pumped by a 404-nm laser diode to produce spontaneous parametric down-conversion and a half-wave plate (HWP) with the setting angle $\theta = \frac{1}{2}\arcsin a$, we can produce photon pairs in the family of entangled states

$$|\phi\rangle = a|HH\rangle + \sin(\arccos a)|VV\rangle, \tag{10}$$

where H and V represent horizontal and vertical polarizations, respectively. Fidelities of the states are about 97%.

Concurrence of the states are obtained from the reconstructed density matrices via fully state tomography[36]. The polarization of each photon is analysed on an arbitrary basis, by means of a quarter-wave plate (QWP), HWP, and a polarizing beam splitter (PBS) in each arm. Making 16 measurements of the polarization correlations in various bases allows tomographic reconstruction of the density matrix of the two-photon states. Photons are detected in coincidence using silicon avalanche photodiodes (APDs), thereby projecting out the large vacuum state from the possibility of the pump photon not downconverting, and selecting the two-photon contribution to quantum states. Photon counts are taken

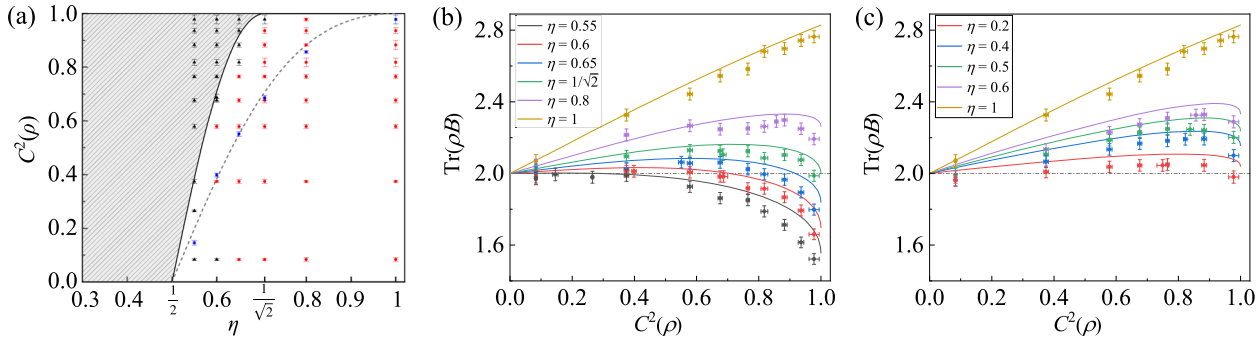

Fig. 2 Experimental results for the first and second scenarios. a Squared concurrence of the state $C^2(\rho)$ versus the detection efficiency of Bob's noisy measurement η. For a given η, a state with the squared concurrence at or above the solid curve (the shaded area) will never violate the CHSH inequality. For $\eta > 1/2$, there is always a state violating the CHSH inequality maximally and the squared concurrence of the state is given by the dashed curve. For $\eta \leq 1/\sqrt{2}$, no maximally entangled states ($C^2 = 1$) can violate the CHSH inequality. In our experiment, more values of η in $(1/2, 1/\sqrt{2}]$ are chosen to manifest the behavior around $\eta = 1/\sqrt{2}$. Black triangles denote the squared concurrence of the states which do not violate the CHSH inequality for a given η. Red dots denote C^2 of the states which violate the CHSH inequality. Blue squares denote C^2 of the states which violate the CHSH inequality maximally. **b** Violations of the CHSH inequality versus the squared concurrences of the states for various detection efficiency η. For $\eta < 1$, more nonlocality with less entanglement is observed. **c** Violations of the CHSH inequality versus the squared concurrences of the states for the second scenario, where only one of Bob's measurement choices is inefficient. The CHSH inequality can be violated for an arbitrary $\eta > 0$. To show the difference between the first and second scenarios, we choose more values of η in $[0, 1/2]$. Error bars indicate the statistical uncertainty which is obtained based on assuming Poissonian statistics.

to be fair samples of the true probabilities for obtaining each outcome for every preparation-measurement pair.

To test the CHSH inequality, one of the photons is sent to Bob for his noisy measurement and the other is for Alice's perfect measurement. For Alice's side, the measurement of her observable O_x^A is a standard polarization measurement using an HWP at θ_A and a PBS. The HWP is used to map the eigenstate of the observable corresponding to the eigenvalue 1 into $|H\rangle$ and the PBS is for projective measurement of the observable σ_z—one of the standard Pauli operators. Two outcomes are read by APDs (D_{A0} and D_{A1}).

In the first scenario, Bob performs a POVM $\{\tilde{\Pi}^B_{0|y}, \tilde{\Pi}^B_{1|y}\}$ instead of projective measurement[37–43]. He needs two steps to implement the two-outcome measurements. First, a projector (the first term of $\tilde{\Pi}^B_{0|y}$ or $\tilde{\Pi}^B_{1|y}$) is realized by an HWP at θ_B. Then partially projecting polarizing elements involving two birefringent calcite beam displacers (BDs) and two HWPs to produce the required projectors with the appropriate weights, which are encoded into the angle of one of the HWPs $\theta_\eta = \arccos\sqrt{\eta}/2$ (η is the efficiency of the noisy measurement which is simulated here via the optical implementation of the POVM). Two outcomes of Bob's measurement are read by APDs (D_{B0} and D_{B1}). The conditional probability $p(a, b|x, y)$, which denotes the probability obtained in the case Alice chooses to measure her qubit in the direction $\hat{a}_x$ and the outcome is a, while Bob chooses to measure his qubit in the direction $\hat{b}_y$ with inefficient detectors and the outcome is b, is obtained by the coincidence counts $N(a, b|x, y)$ between APDs (D_{Aa},D_{Bb}) normalizing by the total photon counts. For example, $p(0, 0|1, 1) = N(0, 0|1, 1)/\Sigma_{a,b}N(a, b|1,1)$. For the second scenario, Bob performs a projective measurement (1) for $y = 0$ and a POVM (2) for $y = 1$ via the above setups, respectively. All the measurement events on Bob's side need to be heralded by Alice's detectors.

Experimental results for the first scenario are shown in Fig. 2a, b. We choose six different settings $\eta = 0.55, 0.6, 0.65, 1/\sqrt{2}, 0.8, 1$ for the noisy measurement. For each η, we choose a family of two-qubit states $|\phi\rangle$(10) with squared concurrences 0.1, 0.4, 0.6, 0.7, 0.8, 0.86, 0.92, 0.96, 1, respectively. Then we optimize the measurement directions $\{\hat{a}_0, \hat{a}_1, \hat{b}_0, \hat{b}_1\}$ for violating the CHSH inequality. In addition to the above states with fixed squared concurrences, we also choose the states which violate the CHSH inequality maximally, for each η.

In Fig. 2a, the solid line signifies the upper bound on the amount of entanglement needed to violate the CHSH inequality for a given η. The states with the squared concurrences at or above the solid line (the shadow area) do not violate the CHSH inequality. For $\eta > 1/2$, there always exists a state maximally violating the CHSH inequality, and the squared concurrence of this state is given by the dashed line obtained theoretically. For $\eta \leq 1/\sqrt{2}$, no maximally entangled states ($C^2 = 1$) can violate the CHSH inequality.

In Fig. 2b, we show the value of the CHSH violation versus the squared concurrence for the first scenario. For $\eta = 1$, the value of the CHSH violation increases with the squared concurrence linearly and the maximal entangled state $|\Phi^+\rangle = (|00\rangle + |11\rangle)/\sqrt{2}$ violates the CHSH inequality with $\mathrm{Tr}(|\Phi^+\rangle\langle\Phi^+|\mathcal{B}_1) = 2.7629 \pm 0.0337$ by 22 standard deviations. Surprisingly, for $1/2 < \eta < 1$, as the detection efficiency η decreases, more nonlocality with less entanglement is observed, which agrees with the theoretical prediction in ref. [30]. For example, for $\eta = 0.8$, the state $0.7603|00\rangle + 0.6495|11\rangle$ with squared concurrence 0.8568 ± 0.0048 violates the CHSH inequality with $\mathrm{Tr}(\rho\mathcal{B}_1) = 2.2911 \pm 0.0323$ by nine standard deviations. Whereas, the maximally entangled state violates the CHSH inequality with 2.1938 ± 0.0316 by only six standard deviations.

Experimental results of the second scenario are shown in Fig. 2c. For the POVM of Bob's side, we choose 5 different settings $\eta = 0.2$, 0.4, 0.5, 0.6, 1. For each η, five different two-qubit states $|\phi\rangle$(10) whose squared concurrences are 0.1, 0.4, 0.6, 0.7, 0.8, 0.92, 1, respectively, are chosen. For each η and $|\phi\rangle$, we optimize the directions of measurement for both sides $\{\hat{a}_0, \hat{a}_1, \hat{b}_0, \hat{b}_1\}$ to obtain the maximal violation of the CHSH inequality. Furthermore, we also choose the states which violate the CHSH inequality maximally for each η. Similar to the first scenario, except for the case of $\eta = 1$, as the detection efficiency η decreases, more nonlocality with less entanglement is observed. Take $\eta = 0.6$ as an example, the state $0.8018|00\rangle + 0.5976|11\rangle$ with squared concurrence of 0.8568 ± 0.0167 violates the CHSH inequality with $\mathrm{Tr}(\rho\mathcal{B}_1) = 2.3257 \pm 0.0330$ by ten standard deviations. While the maximally entangled state violates the CHSH inequality with 2.2879 ± 0.0334 by only nine standard deviations. In addition, different from that in the first scenario, the CHSH inequality can always be violated for an arbitrary small $\eta > 0$ in the second scenario.

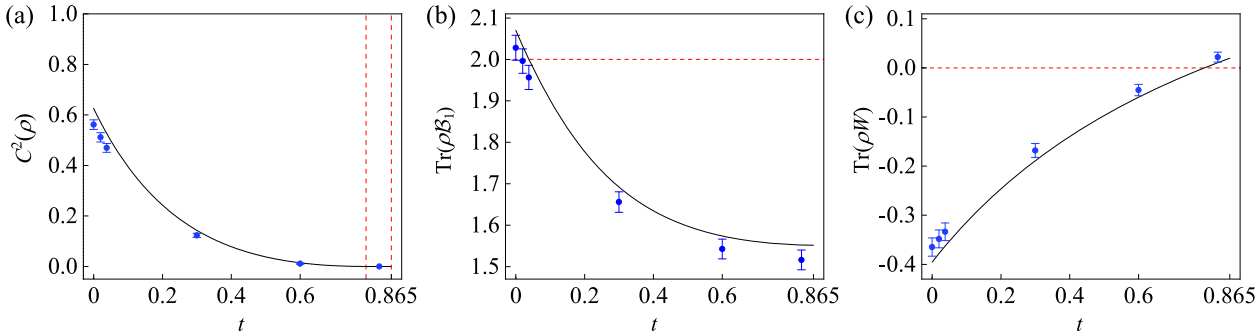

Fig. 3 Experimental results for detecting weak entanglement. a Squared concurrence versus the parameter t of a two-qubit state. For small $0 \le t < 0.791$, ρ is entangled as squared concurrence $C^2(\rho) > 0$. For $0.791 \le t \le 0.865$, ρ is separated as $C^2(\rho) = 0$. **b** Violations of the CHSH inequality versus t. The other parameters of the state and the detection efficiency are fixed as $s = 1/50$, $\tau = 1/2$, and $\eta = 3/4$. Bell nonlocal states with $0 \le t \le 0.038$ violate the CHSH inequality. **c** Values of the entanglement witness $\mathrm{Tr}(\rho W)$ versus t. Entangled Bell local states with $0.038 < t < 0.791$ can be indicated via the entanglement witness. Symbols are experimental data, which agree with their theoretical predictions (solid curves).

Detecting weak entanglement

Furthermore, we theoretically propose and experimentally demonstrate how the CHSH test with noisy measurements can be used to detect the weak entanglement of a two-qubit system. Consider a two-qubit state

$$\rho = \frac{1}{1+t}\left(\frac{|\tilde{\phi}\rangle\langle\tilde{\phi}| + s\mathbb{1}\otimes\mathbb{1}}{1+4s} + t|\tilde{\Phi}^-\rangle\langle\tilde{\Phi}^-|\right), \tag{11}$$

where $|\tilde{\phi}\rangle = \lambda_+|\tilde{0}\tilde{0}\rangle + \lambda_-|\tilde{1}\tilde{1}\rangle$ and $|\tilde{\Phi}^-\rangle = (|\tilde{0}\tilde{0}\rangle - |\tilde{1}\tilde{1}\rangle)/\sqrt{2}$ with $\{|\tilde{0}\rangle, |\tilde{1}\rangle\}$ being the Schmidt basis of $|\phi_0\rangle$ and $\lambda_\pm$ being the Schmidt coefficients. $|\phi_0\rangle$ is the eigenstate of $\mathcal{B}_1$ with the directions of the measurements $\theta_A = 0$ and $\theta_B = \arcsin[(1-\tau)^2/(1+\tau)^2]$. ρ is weakly entangled with a monotonically decreasing squared concurrence $C^2(\rho)$ as parameter t varies among the interval

$$t \in \left[0, \frac{\sqrt{2}\tau - 2s\sqrt{1+\tau^2}}{\sqrt{1+\tau^2}(1+4s)}\right), \tag{12}$$

and has an expected value $\mathrm{Tr}(\rho\mathcal{B}_1) > 2$ if

$$t < 2\frac{1+4s-\sqrt{1+\tau^2}}{(1+4s)(-2-\sqrt{2}\tau)+\sqrt{1+\tau^2}}$$

and

$$s \in \left[0, \frac{1}{4}(\sqrt{1+\tau^2}-1)\right].$$

While, for values of t outside of the interval Eq. (12), ρ may exist stronger entanglement but with no violation of the CHSH equation. Figure 4 gives an intuitive presentation of such a situation, which is discussed in detail in the Method part. Such a property can be used to detect only nonlocal states with weak entanglement.

For experimental demonstration, we fix the detection efficiency of Bob's measurement $\eta = 3/4$. We choose total six values of $t = 0$, 0.02, 0.038, 0.3, 0.6, 0.83 and generate six states with various parameters t and fixed $s = 1/50$ and $\tau = 1/2$[44]. In the measurement stage, the setup is as same as that for the pure state testing the CHSH inequality $\mathcal{B}_1$.

Experimental results are shown as symbols in Fig. 3. In Fig. 3a, for small $t \in [0, 0.791)$, ρ is entangled as its squared concurrence $C^2(\rho) > 0$ and $C^2(\rho)$ decreases with t. For $t \in [0.791, 0.865]$, ρ is separable since $C^2(\rho) = 0$.

In Fig. 3b, weak entanglement is achieved for small t. The violation of the CHSH inequality is even larger than that obtained by the state with more entanglement (with larger t), which can be seen by comparing Fig. 4a, b. For $t \in [0, 0.038]$, $\mathrm{Tr}(\rho\mathcal{B}_1)$ is larger than 2. The CHSH inequality is then violated for these states, which indicates Bell nonlocal states. For example, for $t = 0$, the state has only weak entanglement with the squared concurrence $C^2(\rho) = 0.5617 \pm 0.0190$. However, a violation of the CHSH inequality is still observed for $\mathrm{Tr}(\rho\mathcal{B}_1) = 2.0281 \pm 0.0301$. (Ideally, for $t = 0$ our method still allows to demonstrate nonlocality by violating the CHSH inequality (2.0704). However, the experimental result 2.0281 ± 0.0301 shows that if the error bar is considered the method is not always valid.). Actually, due to the squared concurrences in Fig. 3a, the states with $t \in [0, 0.791)$ are entangled. However, a violation of the CHSH inequality is only observed as $\mathrm{Tr}(\rho\mathcal{B}_1)$ between 2.070 and 2 (theoretical predictions) for $t \in [0, 0.038]$. The interval of separability will be pushed left on the graph for smaller values of s and τ; causing a violation to occur for only small values of parameter t.

The states belonging to the gap between the Bell nonlocal states with $t \in [0, 0.038]$ and the separable states with $t \in [0.791, 0.865]$ are so-called entangled Bell local states, which can be detected via entanglement witnesses[45]. An entanglement witness operator W acting on a bipartite system can be defined via Peres criterion as

$$W = \frac{1}{2}\mathbb{1} - |\tilde{\Phi}^+\rangle\langle\tilde{\Phi}^+|, |\tilde{\Phi}^+\rangle = (|\tilde{0}\tilde{0}\rangle + |\tilde{1}\tilde{1}\rangle)/\sqrt{2}. \tag{13}$$

For separable states, $\mathrm{Tr}(\rho W) \ge 0$, while for entangled states, $\mathrm{Tr}(\rho W) < 0$. In Fig. 3c, it is shown that $\mathrm{Tr}(\rho W) < 0$ for $t \in [0, 0.791)$, which indicates both Bell nonlocal states and entangled Bell local states can be detected by the entanglement witness.

DISCUSSION

Entanglement is a strong nonlocal correlation and an important resource in the development of technologies and protocols exploiting the properties of quantum systems[46,47]. Nonlocality inequalities set a bound on the possible strength of nonlocal correlations. Quantum mechanics predicts the existence of entangled states which violate a nonlocality inequality. Previous attempts to experimentally test nonlocality have all presumed unphysical idealizations that do not hold in real experiments, namely, noiseless measurements. In this work, we perform an experimental violation of the CHSH test that is free of the idealizations and rule out local models with high confidence in two scenarios. For the first scenario, we experimentally demonstrate that the CHSH inequality can always be violated for any efficiency $\eta > 1/2$ which was originally pointed out by[48,49]. We furthermore test the upper bound on the amount of entanglement needed to violate the CHSH inequality for a given η.

Besides, we experimentally study a scenario, which was not previously considered in the literature. We show that the CHSH inequality can always be violated for any nonzero noise parameter of the measurement. Less entanglement exhibits more nonlocality in both of the scenarios. We also provide an application of testing the CHSH inequality with a noisy measurement; that is, the detection of weak entanglement of a two-qubit state. This approach has possible applications for scientific fields wherein quantum effects are important and for developing quantum technologies. For instance, we particularly expect to further develop it for the construction of entanglement witness that only detects nonlocal states with low entanglement.

METHODS

Detailed explanation of the experimental results

Experimental results show that for $\eta \leq 1/\sqrt{2}$, no maximally entangled states ($C^2 = 1$) can violate the CHSH inequality. It is straightforward to show why this is true. Note that we can write the expected value $\mathrm{Tr}(\rho\mathcal{B}_1)$ as

$$\eta \cdot 2\left[(\hat{c}_0, \mathcal{T}_\rho \hat{b}_0)\cos(\theta) + (\hat{c}_1, \mathcal{T}_\rho \hat{b}_1)\sin(\theta)\right] + (1-\eta)\cdot 2(\hat{c}_0\cos(\theta) + \hat{c}_1\sin(\theta), \vec{r}) \tag{14}$$

for measurements $\{\hat{c}_0, \hat{c}_1, \hat{b}_0, \hat{b}_1\}$, Alice's local Bloch vector $\vec{r}$, and the correlation matrix $\mathcal{T}_\rho$. Since a maximally entangled state has local maximally mixed subsystems, the local Bloch vectors must both be zero for Alice and Bob. So the second term vanishes and we are left with the original term Horodecki et al. obtained in ref. [50] with a factor of η. Therefore, the maximum expected value has to be $2\eta\sqrt{\lambda_1 + \lambda_2}$, where λ_1, λ_2 are the largest eigenvalues of the symmetric matrix $\mathcal{T}_\rho^T\mathcal{T}_\rho$. Due to the positivity of maximally entangled two-qubit states[51], both eigenvalues must be unit which gives the optimal value of $2\eta\sqrt{2}$. So maximally entangled states can only violate the CHSH inequality when $\eta > 1/\sqrt{2}$ as suggested by the experimental results.

Details on the proposal of detecting weak entanglement

We theoretically propose and experimentally demonstrate how CHSH tests with noisy measurements can be used to detect weak entanglement on two-qubit states. Consider a two-qubit state ρ in Eq. (11) of the main text. It has an expected value $\mathrm{Tr}(\rho\mathcal{B}_1) > 2$ if

$$t < 2\frac{1+4s-\sqrt{1+\tau^2}}{(1+4s)(-2-\sqrt{2}\tau)+\sqrt{1+\tau^2}}, \quad s \in \left[0, \tfrac{1}{4}(\sqrt{1+\tau^2}-1)\right], \tag{15}$$

where $|\tilde{\phi}\rangle = \lambda_+|\tilde{0}\tilde{0}\rangle + \lambda_-|\tilde{1}\tilde{1}\rangle$ and $|\tilde{\Phi}^-\rangle = (|\tilde{0}\tilde{0}\rangle - |\tilde{1}\tilde{1}\rangle)/\sqrt{2}$ with $\{|\tilde{0}\rangle, |\tilde{1}\rangle\}$ being the Schmidt basis of $|\phi_0\rangle$ and $\lambda_\pm$ being the Schmidt numbers. The state

$$|\phi_0\rangle = \frac{\sqrt{\tau}}{\sqrt{2(1+\tau)(1+\tau^2-\tau\sqrt{1+\tau^2})}}\left[\frac{-1+\tau-\sqrt{1+\tau^2}}{\sqrt{2}\tau}|00\rangle + (\tau-\sqrt{1+\tau^2})|01\rangle + \frac{-1-\tau+\sqrt{1+\tau^2}}{\sqrt{2}\tau}|10\rangle + |11\rangle\right] \tag{16}$$

with $\{|0\rangle, |1\rangle\}$ being the computational basis, is the eigenstate of $\mathcal{B}_1$ corresponding to the eigenvalue $2\sqrt{1+\tau^2}$ ($\tau = 2\eta - 1$) with the directions of the measurements $\theta_A = 0$ and $\theta_B = \arcsin[(1-\tau)^2/(1+\tau)^2]$. The Schmidt numbers are $\lambda_\pm = \sqrt{\pm(1-\tau)+\sqrt{1+\tau^2}}/\sqrt{2\sqrt{1+\tau^2}}$. By doing the singular value decomposition of the matrix form of $|\phi_0\rangle$, given by the isomorphism between four vectors and 2×2 matrices, we are able to obtain the transformation $|\tilde{\phi}\rangle = \mathbb{1}\otimes\mathcal{V}|\phi_0\rangle$ by the use of a local rotation $\mathcal{V}$ which is defined in the computational basis as

$$\mathcal{V} = \frac{1}{\sqrt{2(1+\tau)}}\begin{pmatrix} -\sqrt{1+\tau+\sqrt{1+\tau^2}} & -\sqrt{1+\tau-\sqrt{1+\tau^2}} \\ -\sqrt{1+\tau-\sqrt{1+\tau^2}} & \sqrt{1+\tau+\sqrt{1+\tau^2}} \end{pmatrix}. \tag{17}$$

The concurrence of the state $|\tilde{\phi}\rangle$ can be calculated as $C = 2|\lambda_+\lambda_-| = \sqrt{\frac{2\tau}{1+\tau^2}}$.

For experimental demonstration, we fix the detection efficiency of Bob's measurement at $\eta = 3/4$. For simplification, we generate the state

$$\rho' = \frac{1}{1+t}\left[\frac{1}{1+4s}(|\phi\rangle\langle\phi| + s\mathbb{1}\otimes\mathbb{1}) + t|\Phi^-\rangle\langle\Phi^-|\right] \tag{18}$$

in the computational basis with $|\phi\rangle = \lambda_+|00\rangle + \lambda_-|11\rangle$ and $|\Phi^-\rangle = (|00\rangle - |11\rangle)/\sqrt{2}$ and the desired state ρ can be obtained by a change of basis, i.e., $\rho = \mathbb{1}\otimes\mathcal{V}\rho'\mathbb{1}\otimes\mathcal{V}$. We choose a total of six values of $t = 0$, 0.02, 0.038, 0.3, 0.6, 0.83 to generate six different states and fixed $s = 1/50$ and $\tau = 1/2$.

In the measurement stage, for Alice's side, the setup is the same as that for the pure state testing of the CHSH inequality. For Bob's side, an extra unitary transformation $\mathcal{V}^\dagger\tilde{\Pi}^\beta_{b|y}\mathcal{V}$ is applied to perform a change of basis[52,53]. This unitary combines with another rotation that maps the eigenstate of the observable O^β_y, corresponding to the eigenvalue 1, into $|H\rangle$ and is realized by the HWP at θ_B. The rest is the same as that for the pure state testing of the CHSH inequality associated with the Bell operator $\mathcal{B}_1$.

Experimental results are shown in Fig. 4. The parameters of the state and the detection efficiency are fixed as $s = 1/50$, $\tau = 1/2$, and $\eta = 3/4$. For $0 \leq t < 0.791$ and $t > 0.865$, ρ is entangled as squared concurrence $C^2(\rho) > 0$. For $0.791 \leq t \leq 0.865$, ρ is separated as $C^2(\rho) = 0$. Bell nonlocal states with $0 \leq t \leq 0.038$ and $t > 13.428$ violate the CHSH inequality. For small $t = 0$, the state has only weak entanglement with the squared concurrence $C^2(\rho) = 0.5617 \pm 0.0190$. However, a violation of the CHSH inequality is observed for $\mathrm{Tr}(\rho\mathcal{B}_1) = 2.0281 \pm 0.0301$. For larger $t = 30$, the state with stronger entanglement $C^2(\rho) = 0.8116 \pm 0.0239$ and it violates the CHSH inequality by the value $\mathrm{Tr}(\rho\mathcal{B}_1) = 2.0083 \pm 0.0310$. The violation is even smaller. Thus, we can use the violation of the CHSH inequality with noisy measurements to detect weak measurements.

For the entanglement witness, in our experiment, as we actually generate the state ρ', we measure $\mathrm{Tr}(\rho' W')$ which is equivalent to $\mathrm{Tr}(\rho W)$, where $W' = \frac{1}{2}\mathbb{1} - |\Phi^+\rangle\langle\Phi^+|$ and $|\Phi^+\rangle = (|00\rangle + |11\rangle)/\sqrt{2}$.

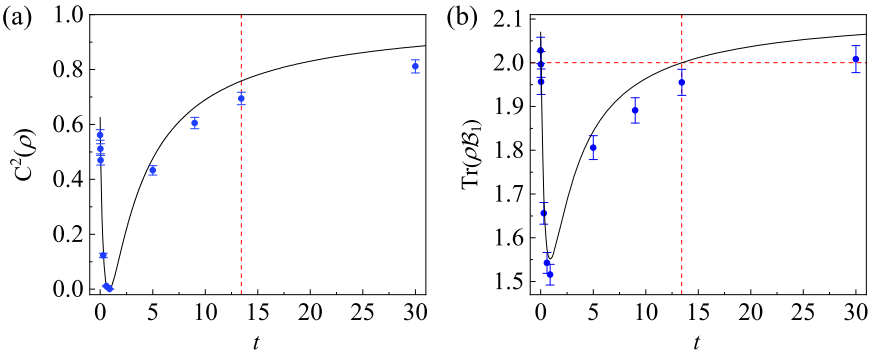

Fig. 4 Experimental results of concurrence and violations of the CHSH inequality. a Squared concurrence versus the parameter t of a two-qubit state. For $0 \leq t < 0.791$ and $t > 0.865$, ρ is entangled as squared concurrence $C^2(\rho) > 0$. For $0.791 \leq t \leq 0.865$, ρ is separated as $C^2(\rho) = 0$. **b** Violations of the CHSH inequality versus t. The other parameters of the state and the detection efficiency are fixed as $s = 1/50$, $\tau = 1/2$, and $\eta = 3/4$. Bell nonlocal states with $0 \leq t \leq 0.038$ and $t > 13.428$ violate the CHSH inequality. Symbols are experimental data, which agree with their theoretical predictions (solid curves).

Experimental implementation of POVMs

To quantify the quality of the experimental realization of the POVMs, we define a modified two-norm distance[38] between the experimentally reconstructed matrix G_{exp} and the ideal one G_{th} as

$$D(G_{exp}, G_{th}) = \sqrt{\frac{\mathrm{Tr}\left[(G_{exp} - G_{th})^2\right]}{\mathrm{Tr}(G_{th}^2)}}. \quad (19)$$

The value of the distance ranges between 0 for a perfect match and $\sqrt{2}$ for a complete mismatch. To reconstruct the matrix form of G_{exp}, we perform the measurement tomography[54]. More specifically, single photons are prepared in four testing states $|H\rangle$, $|V\rangle$, $|R\rangle = (|H\rangle + i|V\rangle)/\sqrt{2}$ and $|D\rangle = (|H\rangle + |V\rangle)/\sqrt{2}$, and are detected by APDs in coincidence with the trigger photons after passing through the optical setup for realizing a certain POVM element. Photon counts give the measured probabilities. From these, we can obtain the matrix forms of all the elements of the POVMs via maximum-likelihood estimation. In our experiment, all the distances turn out to be smaller than 0.03, which validates the experimental realizations of the POVMs.

Experimental generation of mixed states

To detect weak entanglement, we generate mixed state ρ'(18) and fix the parameters as $s = 1/50$, $\kappa = 1/2$, and $\eta = 3/4$. The mixed state is then $\rho' = \frac{1}{1+t}(\frac{25}{27}|\phi\rangle\langle\phi| + \frac{1}{54}\mathbb{1} + t|\Phi^-\rangle\langle\Phi_-|)$, where $|\phi\rangle = 0.851|00\rangle + 0.526|11\rangle$. We generate the two-photon pure entangled states and introduce quantum noise in a controlled way on one of the state subsystems[55,56]. As illustrated in Fig. 1 of the main text, by tuning the setting angle θ_1 of the HWP, we can generate two-photon pure entangled states with real coefficients. For example, with $\theta_1 = \frac{1}{2}\arccos(0.526)$, $|\phi\rangle$ is generated via type-I spontaneous parametric down-conversion using two BBO crystals. By introducing quantum noise through a depolarizing channel $\varepsilon(\rho) = (1 - 3p/4)\rho + p(\sigma_x\rho\sigma_x + \sigma_y\rho\sigma_y + \sigma_z\rho\sigma_z)/4$, we can also generate a Werner state $\rho_W = (1-p)|\Phi^-\rangle\langle\Phi^-| + p\mathbb{1}/4$. The depolarizing channel is introduced in a controlled way by employing two liquid crystal retarders (LCs) in the path of photon A. The LCs act as phase retarders, with the relative phase between the ordinary and extraordinary radiation components depending on the applied voltage. Precisely, V_π and V_1 correspond to the case of LCs operating as HWP and as the identity operator, respectively. The two LCs' optical axes are set at 0° and 45° with respect to the V polarization. Then, when the voltage is applied, one of the LC acts as a σ_z on the single-qubit and the other as σ_x. The simultaneous application of V_π on both LCs corresponds to the σ_y operation. By controlling the activation time and the period of the LCs activation cycle, we can generate the Werner state ρ_W with an arbitrary coefficient. Thus, we generate the pure entangled state $|\phi\rangle$ and the Werner state ρ_W respectively, and then by choosing different exposure time for each state, i.e., the time for coincidence measurement for each state, we can generate the mixed state ρ'. The ratio between exposure times for $|\phi\rangle$ and ρ_W is $\frac{25}{27} : (\frac{2}{27} + t)$.

DATA AVAILABILITY

Any related experimental background information not mentioned in the text and other findings of this study are available from the corresponding author upon reasonable request.

Received: 26 March 2021; Accepted: 12 November 2021;
Published online: 06 December 2021

REFERENCES

1. Einstein, A., Podolsky, B. & Rosen, N. Can quantum-mechanical description of physical reality be considered complete? *Phys. Rev.* **47**, 777 (1935).
2. Bell, J. S. On the Einstein Podolsky Rosen paradox. *Physics* **1**, 195 (1964).
3. Nielsen, M. A. & Chuang, I. L. *Quantum Computation and Quantum Information* (Cambridge Univ. Press, 2000).
4. Bennett, C. H. & Brassard, G. Quantum cryptography: public key distribution and coin tossing. *Theor. Computer Sci.* **560**, 7 (2014).
5. Ekert, A. K. Quantum cryptography based on Bell's theorem. *Phys. Rev. Lett.* **67**, 661 (1991).
6. Bennett, C. et al. Teleporting an unknown quantum state via dual classical and Einstein-Podolsky-Rosen channels. *Phys. Rev. Lett.* **70**, 1895 (1993).
7. Horodecki, R., Horodecki, M. & Horodecki, P. Teleportation, Bell's inequalities and inseparability. *Phys. Lett. A* **222**, 21 (1996).
8. Gisin, N., Ribordy, G., Tittel, W. & Zbinden, H. Quantum cryptography. *Rev. Mod. Phys.* **74**, 145 (2002).
9. Eberhard, P. H. Background level and counter efficiencies required for a loophole-free Einstein-Podolsky-Rosen experiment. *Phys. Rev. A* **47**, R747 (1993).
10. Hardy, L. Nonlocality for two particles without inequalities for almost all entangled states. *Phys. Rev. Lett.* **71**, 1665 (1993).
11. Acín, A., Durt, T., Gisin, N. & Latorre, J. I. Quantum nonlocality in two three-level systems. *Phys. Rev. A* **65**, 052325 (2002).
12. Brunner, N., Gisin, N. & Scarani, V. Entanglement and non-locality are different resources. *N. J. Phys.* **7**, 88 (2005).
13. Cabello, A. & Larsson, J.-A. Minimum detection efficiency for a loophole-free atom-photon Bell experiment. *Phys. Rev. Lett.* **98**, 220402 (2007).
14. Brunner, N., Gisin, N., Scarani, V. & Simon, C. Detection loophole in asymmetric Bell experiments. *Phys. Rev. Lett.* **98**, 220403 (2007).
15. Buhrman, H., Cleve, R., Massar, S. & Wolf, R. Nonlocality and communication complexity. *Rev. Mod. Phys.* **82**, 665–698 (2010).
16. Pál, K. F. & Vértesi, T. Maximal violation of a bipartite three-setting, two-outcome Bell inequality using infinite-dimensional quantum systems. *Phys. Rev. A* **82**, 022116 (2010).
17. Vidick, T. & Wehner, S. More nonlocality with less entanglement. *Phys. Rev. A* **83**, 052310 (2011).
18. Junge, M. & Palazuelos, C. Large violation of Bell inequalities with low entanglement. *Math. Phys.* **306**, 695 (2011).
19. Liang, Y.-C., Vértesi, T. & Brunner, N. Large semi-device-independent bounds on entanglement. *Phys. Rev. A* **83**, 022108 (2011).
20. Christensen, B. G., Liang, Y.-C., Brunner, N., Gisin, N. & Kwiat, P. G. Exploring the limits of quantum nonlocality with entangled photons. *Phys. Rev. X* **5**, 041052 (2015).
21. Fonseca, E. A. & Parisio, F. Measure of nonlocality which is maximal for maximally entangled qutrits. *Phys. Rev. A* **92**, 030101(R) (2015).
22. Lipinska, V., Curchod, F. J., Máttar, A. & Acín, A. Towards an equivalence between maximal entanglement and maximal quantum nonlocality. *N. J. Phys.* **20**, 063043 (2018).
23. Hagley, E. et al. Generation of Einstein-Podolsky-Rosen pairs of atoms. *Phys. Rev. Lett.* **79**, 1–5 (1997).
24. Ansmann, M. et al. Violation of Bell's inequality in Josephson phase qubits. *Nature* **461**, 504–506 (2009).
25. Dada, A. C., Leach, J., Buller, G. S., Padgett, M. J. & Andersson, E. Experimental high-dimensional two-photon entanglement and violations of generalized Bell inequalities. *Nat. Phys.* **7**, 677–680 (2011).
26. Pan, J. W. et al. Multiphoton entanglement and interferometry. *Rev. Mod. Phys.* **84**, 777 (2012).
27. Tan, T. R. et al. Multi-element logic gates for trapped-ion qubits. *Nature* **528**, 380 (2015).
28. Rowe, M. A. et al. Experimental violation of a Bell's inequality with efficient detection. *Nature* **409**, 791–794 (2001).
29. Clauser, J. F., Horne, M. A., Shimony, A. & Holt, R. A. Proposed experiment to test local hidden-variable theories. *Phys. Rev. Lett.* **23**, 880 (1969).
30. Dilley, D. & Chitambar, E. More nonlocality with less entanglement in Clauser-Horne-Shimony-Holt experiments using inefficient detectors. *Phys. Rev. A* **97**, 062313 (2018).
31. Hensen, B. et al. Loophole-free Bell inequality violation using electron spins separated by 1.3 kilometres. *Nature* **526**, 682–686 (2015).
32. Cao, Y. et al. Bell test over extremely high-loss channels: towards distributing entangled photon pairs between earth and the moon. *Phys. Rev. Lett.* **120**, 140405 (2018).
33. Li, M. et al. Test of local realism into the past without detection and locality loopholes. *Phys. Rev. Lett.* **121**, 080404 (2018).
34. Abellán, C. et al. Challenging local realism with human choices. *Nature* **557**, 212–216 (2018).
35. Zhan, X. et al. Realization of the contextuality-nonlocality tradeoff with a qubit-qutrit photon pair. *Phys. Rev. Lett.* **116**, 090401 (2016).
36. James, D. F. V., Kwiat, P. G., Munro, W. J. & White, A. G. Measurement of qubits. *Phys. Rev. A* **64**, 052312 (2001).
37. Bian, Z. et al. Realization of single-qubit positive-operator-valued measurement via a one-dimensional photonic quantum walk. *Phys. Rev. Lett.* **114**, 203602 (2015).
38. Zhan, X. et al. Experimental generalized contextuality with single-photon qubits. *Optica* **4**, 996–971 (2017).
39. Wang, K. K. et al. Entanglement-enhanced quantum metrology in a noisy environment. *Phys. Rev. A* **97**, 042112 (2018).
40. Zhu, G. et al. Experimental orthogonalization of highly overlapping quantum states with single photons. *Phys. Rev. A* **100**, 052307 (2019).

41. Bian, Z. et al. Experimental demonstration of one-sided device-independent self-testing of any pure two-qubit entangled state. *Phys. Rev. A* **101**, 020301(R) (2020).
42. Zhan, X. et al. Experimental quantum cloning in a pseudo-unitary system. *Phys. Rev. A* **101**, 010302(R) (2020).
43. Qu, D. et al. Experimental entropic test of state-independent contextuality via single photons. *Phys. Rev. A* **101**, 060101(R) (2020).
44. Yang, M. et al. Experimental simultaneous learning of multiple nonclassical correlations. *Phys. Rev. Lett.* **123**, 190401 (2019).
45. Horodecki, M., Horodecki, P. & Horodecki, R. Separability of mixed states: necessary and sufficient conditions. *Phys. Lett. A.* **223**, 1 (1996).
46. Xue, P., Sanders, B. C. & Leibried, D. Quantum walk on a line for a trapped ion. *Phys. Rev. Lett.* **103**, 130501 (2009).
47. Xue, P. & Xiao, Y. F. Universal quantum computation in decoherence-free subspace with neutral atoms. *Phys. Rev. Lett.* **97**, 140501 (2006).
48. Cabello, A. & Larsson, J. Minimum detection efficiency for a loophole-free atom-photon Bell experiment. *Phys. Rev. Lett.* **98**, 220402 (2007).
49. Brunner, N., Gisin, N., Scarani, V. & Simon, C. Detection loophole in asymmetric Bell experiments. *Phys. Rev. Lett.* **98**, 220403 (2007).
50. Horodecki, R., Horodecki, P. & Horodecki, M. Exploring the limits of quantum nonlocality with entangled photons. *Phys. Lett. A* **200**, 340 (1995).
51. Gamel, O. Exploring the limits of quantum nonlocality with entangled photons. *Phys. Rev. A* **93**, 062320 (2016).
52. Xue, P. et al. Experimental quantum-walk revival with a time-dependent coin. *Phys. Rev. Lett.* **114**, 140502 (2015).
53. Wang, K. K. et al. Simulating dynamic quantum phase transitions in photonic quantum walks. *Phys. Rev. Lett.* **122**, 020501 (2019).
54. Nie, Y. Q. et al. Experimental measurement-device-independent quantum random-number generation. *Phys. Rev. A* **94**, 060301 (2016).
55. Chiuri, A. et al. Experimental realization of optimal noise estimation for a general Pauli channel. *Phys. Rev. Lett.* **107**, 253602 (2011).
56. Orieux, A. et al. Exploring the limits of quantum nonlocality with entangled photons. *Phys. Rev. Lett.* **111**, 220501 (2013).

ACKNOWLEDGEMENTS

This work has been supported by the National Natural Science Foundation of China (Grant Nos. 12025401 and U1930402).

AUTHOR CONTRIBUTIONS

G.Z. performed the experiments with contributions from K.W. and L.X.; D.D. and E.C. performed the theoretical analysis; P.X. supervised the experiment and wrote the paper with input from all authors.

COMPETING INTERESTS

The authors declare no competing interests.

ADDITIONAL INFORMATION

Correspondence and requests for materials should be addressed to Peng Xue.

Reprints and permission information is available at http://www.nature.com/reprints

Publisher's note Springer Nature remains neutral with regard to jurisdictional claims in published maps and institutional affiliations.